

Calculation of the temperature dependence of the vibrational modes of molybdenum

This article has been downloaded from IOPscience. Please scroll down to see the full text article.

1991 J. Phys.: Condens. Matter 3 9629

(<http://iopscience.iop.org/0953-8984/3/48/005>)

View [the table of contents for this issue](#), or go to the [journal homepage](#) for more

Download details:

IP Address: 171.66.16.159

The article was downloaded on 12/05/2010 at 10:54

Please note that [terms and conditions apply](#).

Calculation of the temperature dependence of the vibrational modes of molybdenum

Y Y Ye†‡, K M Ho†, Y Chen†§ and B N Harmon†

†Ames Laboratory USDOE, and Department of Physics, Iowa State University, Ames, IA 50011, USA

Received 12 June 1991

Abstract. First-principles total energy calculations are used to derive the anharmonic coupling parameters for the phonon–phonon interactions in molybdenum. The calculated frequency shifts from 10 to 295 K are in reasonably good agreement with experiment. The derived anharmonic forces are analysed in terms of a central potential and bond-bending terms which are found to be significant.

1. Introduction

Improvements in computing speed and the development of modern computational methods in the past decade have made routine the first-principles calculation of many material-dependent properties including vibrational frequencies, bulk moduli, cohesive energies, and phase transition pressures [1]. In particular, detailed first-principles studies of selected phonon vibrational modes can be made using precise calculations of the total energy changes associated with atomic displacements [2]. Unlike traditional perturbative methods, this ‘frozen phonon’ method allows the total energy to be calculated for large distortions away from the high symmetry, equilibrium geometry. Thus, accurate information about anharmonic interactions is provided by these calculations; however, extracting this information can be somewhat involved. In this article we use the anharmonic terms derived from total energy calculations to obtain the phonon–phonon coupling strengths for Mo. The temperature dependence of the lattice vibrational modes are then determined and compared with experimental measurements [3–5].

Our calculations for Mo were motivated by the existence of detailed experimental measurements of the phonon spectra of Mo over a wide temperature range (from 4.2 to 1200 K) [5]. Previous first-principles total energy calculations [2, 6] have been successful in giving a good description of the bulk structural properties and the frequencies of some phonon modes in bulk Mo. The calculational procedures used in the present calculation are similar to a previous calculation [7] in which we have examined the anharmonic shifts in the phonon modes of the high temperature BCC phase of Zr. However, unlike the case of Zr, we find that in Mo the anharmonic forces are not well described by a short-range central-force model and we had to include the effects of

‡ Permanent address: Physics Department, Wuhan University, People's Republic of China.

§ Current address: University of Wisconsin, Milwaukee, USA.

bond-bending forces due to the emerging importance of directional bonding as the d band occupation is increased.

2. Method of calculation

The temperature dependence of the phonon frequencies are calculated within the perturbative formalism developed for the treatment of anharmonic effects in crystals [8]. The total crystalline potential energy is expanded through fourth order in a power series in the displacements of the atoms from equilibrium. The lowest-order perturbative expressions include treatment of the third-order expansion coefficient to second order in perturbation theory and first-order perturbative terms involving fourth-order expansion coefficients. For the phonon modes of interest, the unrenormalized harmonic frequency can be obtained from first-principles frozen-phonon calculations and the temperature dependence of the frequency can then be evaluated using the following formula [8]:

$$\begin{aligned} \Delta(m\omega_{q_1\lambda_1}^2) = & \frac{1}{2N} \frac{\hbar}{m\omega_{q_1\lambda_1}} \sum_{q_2\lambda_2} v^{(4)}(q_1\lambda_1, -q_1\lambda_1, q_2\lambda_2, -q_2\lambda_2)(2n_{q_2\lambda_2} + 1) \\ & - \frac{9}{8N} \sum_{q_2\lambda_2} \sum_{q_3\lambda_3} |v^{(3)}(q_1\lambda_1, q_2\lambda_2, q_3\lambda_3)|^2 \frac{\hbar^2}{m^2\omega_{q_2\lambda_2}\omega_{q_3\lambda_3}} \\ & \times \left[\frac{n_{q_2\lambda_2} + n_{q_3\lambda_3} + 1}{\hbar\omega_{q_1\lambda_1} + \hbar\omega_{q_2\lambda_2} + \hbar\omega_{q_3\lambda_3}} + \frac{n_{q_3\lambda_3} - n_{q_2\lambda_2}}{\hbar\omega_{q_1\lambda_1} + \hbar\omega_{q_2\lambda_2} - \hbar\omega_{q_3\lambda_3}} \right. \\ & \left. + \frac{n_{q_2\lambda_2} - n_{q_3\lambda_3}}{\hbar\omega_{q_1\lambda_1} - \hbar\omega_{q_2\lambda_2} + \hbar\omega_{q_3\lambda_3}} - \frac{n_{q_2\lambda_2} + n_{q_3\lambda_3} + 1}{\hbar\omega_{q_1\lambda_1} - \hbar\omega_{q_2\lambda_2} - \hbar\omega_{q_3\lambda_3}} \right] \quad (1) \end{aligned}$$

where m is the atomic mass, $\omega_{q\lambda}$ is the frequency of the λ th phonon mode with wavevector q . The effect of temperature enters through the phonon occupation factors $n_{q\lambda}$. Finally, $v^{(3)}$ and $v^{(4)}$ are the third- and fourth-order anharmonic phonon-phonon coupling matrix elements obtained from an expansion of the crystal energy in powers of the atomic displacements u_i .

To evaluate the frequency shifts of the phonons as a function of temperature, we employed a short-range model for the anharmonic interaction. In this model the anharmonic interactions in Mo are described by a sum of a two-body central potential $\varphi(r)$ and an anharmonic three-body Keating potential v_{bb} [9]. The Keating potential is used in order to include the effects of directional bonding which we found to be important in determining shear elastic constants and the phonon spectrum in Mo [10].

Here we give detailed expressions for the anharmonic coupling parameters used in our model. We assume the crystal has one basis atom per unit cell which is true for the BCC lattice. The central potential is characterized by two parameters d and p : the second derivative of the central potential is given by

$$\varphi'' = d/(r^2)^p. \quad (2)$$

The central potential contributions to $v^{(3)}$ and $v^{(4)}$ are

$$v^{(n)}(q_1\lambda_1 \cdots q_n\lambda_n) = \delta(q_1 + q_2 + \cdots + q_n - G) \sum_{h, \alpha_1 \cdots \alpha_n} \frac{v_{\alpha_1 \cdots \alpha_n}^{(n)}(\mathbf{R}_h)}{n!} e_{\alpha_1}(q_1\lambda_1) \cdots e_{\alpha_n}(q_n\lambda_n) (1 - e^{iq_1 \cdot \mathbf{R}_h}) \cdots (1 - e^{iq_n \cdot \mathbf{R}_h}) \quad (3)$$

where \mathbf{R}_h represents a sum over the real space Bravais lattice vectors. In our calculations, the sum includes terms up to the second nearest neighbours. The α 's indicate the Cartesian directions x , y and z . $\hat{e}(q\lambda)$ is the polarization vector of the $q\lambda$ phonon and $v_{\alpha_1 \cdots \alpha_n}^{(n)}(\mathbf{R}_h)$ are expansion coefficients of the central potential which have the form:

$$\begin{aligned} v_{\alpha\alpha\alpha\alpha} &= -12\varphi'' - 48\varphi''' R_\alpha^2 - 16\varphi'''' R_\alpha^4 \\ v_{\alpha\alpha\beta\beta} &= -4\varphi'' - 8\varphi'''(R_\alpha^2 + R_\beta^2) - 16\varphi'''' R_\alpha^2 R_\beta^2 \\ v_{\alpha\beta\beta\beta} &= -24\varphi''' R_\alpha R_\beta - 16\varphi'''' R_\alpha R_\beta^3 \\ v_{\alpha\beta\gamma\gamma} &= -8\varphi''' R_\alpha R_\beta - 16\varphi'''' R_\alpha R_\beta R_\gamma^2 \end{aligned} \quad (4)$$

for the fourth-order terms, and

$$\begin{aligned} v_{\alpha\alpha\alpha} &= -12\varphi'' R_\alpha - 8\varphi''' R_\alpha^3 \\ v_{\alpha\beta\beta} &= -4\varphi'' R_\alpha - 8\varphi''' R_\alpha R_\beta^2 \\ v_{\alpha\beta\gamma} &= -8\varphi''' R_\alpha R_\beta R_\gamma \end{aligned} \quad (5)$$

for the third-order terms. In equations (4) and (5) the central potential is assumed to be a function of r^2 and the derivatives are taken with respect to r^2 .

The anharmonic bond-bending potential has the form

$$U_{bb} = \frac{1}{2} \sum_o \sum_{i,j} v_{bb}(\xi_{oij}) \quad (6)$$

where

$$\begin{aligned} \xi_{oij} &= (\mathbf{x}_i - \mathbf{x}_o) \cdot (\mathbf{x}_j - \mathbf{x}_o) - (\mathbf{R}_i - \mathbf{R}_o) \cdot (\mathbf{R}_j - \mathbf{R}_o) \\ &= (\mathbf{R}_i - \mathbf{R}_o) \cdot (\mathbf{u}_j - \mathbf{u}_o) + (\mathbf{R}_j - \mathbf{R}_o) \cdot (\mathbf{u}_i - \mathbf{u}_o) + (\mathbf{u}_i - \mathbf{u}_o) \cdot (\mathbf{u}_j - \mathbf{u}_o). \end{aligned} \quad (7)$$

The summation o is over all atoms, and the sum i, j is over all pairs of nearest neighbours of o . \mathbf{R}_i is the equilibrium position of the i th atom and $\mathbf{x}_i = \mathbf{R}_i + \mathbf{u}_i$ is the displaced position of the i th atom. We express the function v_{bb} as a polynomial:

$$v_{bb}(\xi) = A_2 \xi^2 + A_3 \xi^3 + A_4 \xi^4. \quad (8)$$

Using this expression for the anharmonic interaction, we can expand the energy of the crystal in powers of the atomic displacements \mathbf{u} and obtain expressions for the contribution of the bond-bending contributions to $v^{(3)}$ and $v^{(4)}$:

Let $\mathbf{r}_i \equiv \mathbf{R}_i - \mathbf{R}_o$, then

$$\begin{aligned}
 v^{(4)}(q_1\lambda_1, q_2\lambda_2, q_3\lambda_3, q_4\lambda_4) &= \delta(q_1 + q_2 + q_3 + q_4 - G) \sum_{\alpha\beta\gamma\delta} e_\alpha(q_1\lambda_1)e_\beta(q_2\lambda_2)e_\gamma(q_3\lambda_3)e_\delta(q_4\lambda_4) \\
 &\times \sum_{i,j} [v_{iiii}^{\alpha\beta\gamma\delta} (1 - e^{i\mathbf{q}_1 \cdot \mathbf{r}_j})(1 - e^{i\mathbf{q}_2 \cdot \mathbf{r}_j})(1 - e^{i\mathbf{q}_3 \cdot \mathbf{r}_j})(1 - e^{i\mathbf{q}_4 \cdot \mathbf{r}_j}) \\
 &+ v_{iiij}^{\alpha\beta\gamma\delta} (1 - e^{i\mathbf{q}_1 \cdot \mathbf{r}_j})(1 - e^{i\mathbf{q}_2 \cdot \mathbf{r}_j})(1 - e^{i\mathbf{q}_3 \cdot \mathbf{r}_j})(1 - e^{i\mathbf{q}_4 \cdot \mathbf{r}_i}) \\
 &+ v_{ijij}^{\alpha\beta\gamma\delta} (1 - e^{i\mathbf{q}_1 \cdot \mathbf{r}_j})(1 - e^{i\mathbf{q}_2 \cdot \mathbf{r}_i})(1 - e^{i\mathbf{q}_3 \cdot \mathbf{r}_j})(1 - e^{i\mathbf{q}_4 \cdot \mathbf{r}_i})] \quad (9)
 \end{aligned}$$

where the summation i, j is over all pairs of nearest neighbours of o , and

$$v_{iiii}^{\alpha\beta\gamma\delta} = 2r_{i\alpha}r_{i\beta}r_{i\gamma}r_{i\delta}A_4 \quad (10)$$

$$v_{iiij}^{\alpha\beta\gamma\delta} = 8r_{i\alpha}r_{i\beta}r_{i\gamma}r_{j\delta}A_4 + 6r_{i\alpha}r_{i\beta}\delta_{\gamma\delta}A_3 \quad (11)$$

$$v_{ijij}^{\alpha\beta\gamma\delta} = 6r_{i\alpha}r_{j\beta}r_{i\gamma}r_{j\delta}A_4 + 6r_{i\alpha}r_{j\beta}\delta_{\gamma\delta}A_3 + \delta_{\alpha\beta}\delta_{\gamma\delta}A_2. \quad (12)$$

For the third-order terms:

$$\begin{aligned}
 v^{(3)} &= -\delta(q_1 + q_2 + q_3 - G) \sum_{\alpha\beta\gamma} e_\alpha(q_1\lambda_1)e_\beta(q_2\lambda_2)e_\gamma(q_3\lambda_3) \\
 &\times \sum_{ij} [v_{iii}^{\alpha\beta\gamma} (1 - e^{i\mathbf{q}_1 \cdot \mathbf{r}_j})(1 - e^{i\mathbf{q}_2 \cdot \mathbf{r}_j})(1 - e^{i\mathbf{q}_3 \cdot \mathbf{r}_j}) \\
 &+ v_{ijj}^{\alpha\beta\gamma} (1 - e^{i\mathbf{q}_1 \cdot \mathbf{r}_j})(1 - e^{i\mathbf{q}_2 \cdot \mathbf{r}_j})(1 - e^{i\mathbf{q}_3 \cdot \mathbf{r}_i})] \quad (13)
 \end{aligned}$$

with

$$v_{iii}^{\alpha\beta\gamma} = 2r_{i\alpha}r_{i\beta}r_{i\gamma}A_3$$

$$v_{ijj}^{\alpha\beta\gamma} = 6r_{i\alpha}r_{i\beta}r_{j\gamma}A_3 + 2r_{i\alpha}\delta_{\beta\gamma}A_2. \quad (14)$$

Thus within our model, the anharmonic forces in Mo are determined by five parameters d, p, A_2, A_3 and A_4 . The values of these parameters can be determined by fitting to the anharmonic terms we obtained from first-principles frozen-phonon calculations of selected phonon modes.

The first-principles frozen-phonon calculations were performed within the local-density-functional formalism using a first-principles pseudopotential method [1]. The only approximations involve the treatment of the exchange-correlation energy using the local density functional formalism, the frozen core approximation, and the Born-Oppenheimer approximation. Technical details of the calculations were presented in earlier articles [1, 2]. For the analysis of a particular phonon the total energy is evaluated as a function of the magnitude of atomic displacements which are chosen to be in the directions corresponding to the polarization vector of the phonon mode under consideration. With these so called 'frozen-phonon' calculations a complete self-consistent band structure calculation is performed for each lattice configuration

so that the full screening and the electron-phonon coupling are accurately determined. Calculations were performed for the T_1 , T_2 and L phonons at the N-point $((\frac{1}{2}, \frac{1}{2}, 0)$ in units of $2\pi/a$), the L and T phonons at the ω -point, $(\frac{2}{3}, \frac{2}{3}, \frac{2}{3})$, the three-fold degenerate phonon at P, $(\frac{1}{2}, \frac{1}{2}, \frac{1}{2})$, and the L and T phonons at $(\frac{1}{2}, 0, 0)$, (the G-point). The change of the energy for the distorted lattice can be expanded in a power series in the displacements of the atoms

$$\Delta E = a\delta^2 + b\delta^3 + c\delta^4 + \dots \quad (15)$$

The harmonic coefficient, a , and the fourth-order coefficient, c , are conveniently displayed in an E/δ^2 against δ^2 plot. (For many of the phonon modes studied the coefficient b is zero by symmetry. However, in the special case when the wavevector \mathbf{q} of the phonon under consideration satisfies $3\mathbf{q} = \mathbf{G}$ for some reciprocal lattice vector \mathbf{G} , then that mode can have a non-zero third-order self-interaction.) As an example we show in figures 1 and 2 the results of the energy against displacement calculations for two of the N-point modes. The intercept gives a , the harmonic coefficient, and the slope for small δ^2 gives c , the fourth-order coefficient. For the L mode, higher-order terms are evident for large displacements. The numerical precision of these calculations was monitored, and for the T_1 mode convergence required sampling 350 \mathbf{k} -points in the irreducible eighth of the Brillouin zone. Similar grids were used for the T_2 and L phonons at the N-point. 108 \mathbf{k} -points were used for the P-point and the G-point. The grid for the ω -point contained 57 \mathbf{k} s for the L phonon and 56 \mathbf{k} s for the T phonon. Data from the H-point were not included because the presence of a Kohn anomaly at the H-point [11]. The phonon frequencies derived from the harmonic coefficients are only valid at zero temperature.

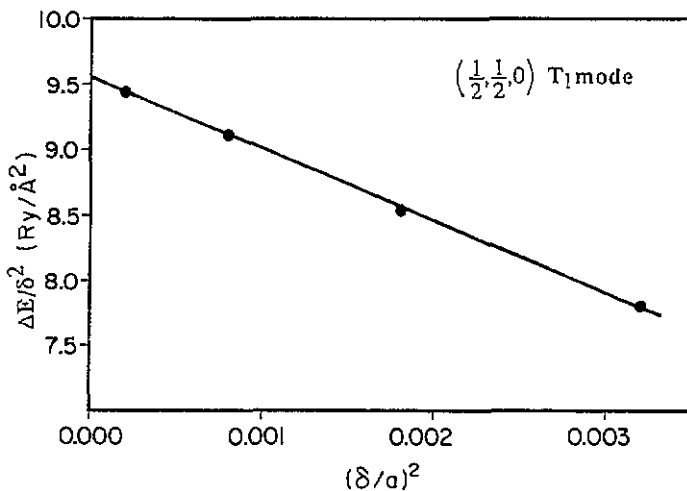


Figure 1. The first-principles total energy against displacement results for the T_1 N-point vibrational of Mo. The results are plotted as $\Delta E/\delta^2$ against δ^2 so that the slope gives the fourth-order anharmonic coefficient. (The lattice constant $a = 3.14$ Å.)

The first-principles calculations are involved and costly, so that only a few selected phonons may be studied via the 'frozen phonon' approach. To extrapolate the first-principles information about anharmonic interactions from a few phonons to the

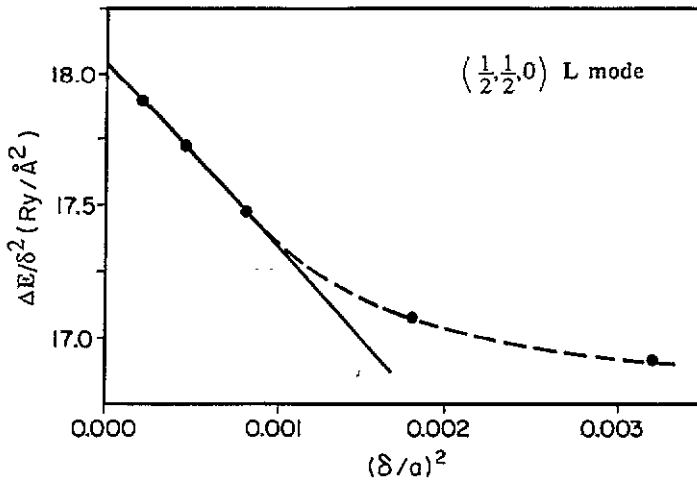


Figure 2. Same as figure 1 but for the longitudinal mode at the N-point. The curvature at larger displacements is evidence for higher-order anharmonic terms.

general anharmonic interactions among all the phonons we used the previously described model. The parameters of the model were determined from a least-squares fit to the fourth-order expansion coefficients derived from the frozen phonon calculations. Table 1 lists the coefficients and the corresponding values from the fitting function. The values of the parameters obtained from the fit were: $d = 4.59 \times 10^5$ Ryd (\AA^2) p , $p = 9.80$, $A_2 = 0.02515 \text{ \AA}^{-4}$, $A_3 = 0.00181 \text{ \AA}^{-6}$, $A_4 = -0.00118 \text{ \AA}^{-8}$. We have also attempted to fit the first-principles anharmonic force constants using only central force terms. For Mo we found that, unlike the previous case of Zr [7], the simple central force model gives a very poor fit to the first-principles results.

Table 1. Values of the calculated harmonic terms (the parameter a in equation (15)), the corresponding harmonic phonon frequencies, and the experimentally measured frequencies at 4.2 K (from [5]). Also given are the calculated fourth-order expansion coefficients (the parameter c in equation (15)) along with the values from the fit to the first-principles results obtained with the model described in the text.

K		c (Ryd \AA^{-2})			Phonon frequency (THz)	
		Cal.	Fit	a (Ryd \AA^{-2})	Cal.	Exp.
$(\frac{1}{2}, \frac{1}{2}, 0)$	L	-3.50	-3.11	0.916	7.94	8.24 ± 0.07
	T_1	-2.83	-2.56	0.485	5.78	—
$(\frac{2}{3}, \frac{2}{3}, \frac{2}{3})$	L	-1.87	-2.11	0.351	6.02	6.14 ± 0.05
	T	+0.18	+0.16	0.459	6.89	7.02 ± 0.06
$(\frac{1}{2}, \frac{1}{2}, \frac{1}{2})$	L, T	+0.25	+0.10	0.289	6.30	6.46 ± 0.06
$(\frac{1}{2}, 0, 0)$	L	+0.08	+0.10	0.365	7.09	7.22 ± 0.05
	T	+0.15	+0.15	0.136	4.33	4.61 ± 0.02

The summations in equation (1) were performed by dividing the Brillouin zone into small cubes with the coupling strengths assumed constant within each cube and the

integration of the energy denominator being performed analytically. To test convergence the number of cubes along Γ to H was varied between 10 and 20. The important fourth-order term was fully converged, while the less significant third-order term was uncertain by $\pm 20\%$.

3. Results

Table 2 shows the results for the phonon frequency shifts from 10.5 to 295 K obtained from our calculations, and compared with the results of neutron scattering measurements. With the exception of the phonon at the H-point, most of the calculated results agree rather well with experiment. At the H-point, (1,0,0), our calculations predicted a large downward shift whereas the experiments showed a small upward rise in phonon frequency with temperature. It is well known that there is a sharp Kohn anomaly for the phonon dispersion curve of Mo at the H-point. The discrepancy between our calculations and experiment are most likely due to thermally caused changes in the sharp Fermi-surface-nesting which are not taken correctly into account within our present calculations [11, 12]. We also predicted that there should be a big downward shift in frequency for the T_1 mode at the N-point. Unfortunately, we have been unable to find any experimental data for comparison at that point. In the table we have also separated the calculated phonon frequency shifts into contributions from the central force, the angular force and thermal expansion. We can see that the thermal expansion contribution is smaller in magnitude than the other two contributions which tend to be opposite in sign: the angular forces cause a softening with increasing temperature whereas the central forces cause a hardening with temperature. Qualitatively similar behaviour was also found in tetrahedral semiconductors [13].

Table 2. The calculated shifts in frequency from 10.5 to 295 K for selected phonons of Mo. The experimental data from [5]. Also listed are the individual theoretical contributions for the anharmonic central and bond-bending forces as well as the volume expansion.

K		Centr	b-b	Vol	$\Sigma_{(THz)}$	Exp _(THz)
$(\frac{1}{2}\frac{1}{2}0)$	L	0.184	-0.154	-0.092	-0.06	-0.11 ± 0.07
	T_1	-0.009	-0.225	-0.025	-0.26	?
	T_2	0.168	-0.120	-0.048	0.00	0.00 ± 0.07
$(\frac{2}{3}\frac{2}{3}\frac{2}{3})$	L	0.036	-0.194	-0.027	-0.19	-0.17 ± 0.05
	T	0.154	-0.162	-0.073	-0.08	-0.18 ± 0.10
$(\frac{1}{2}\frac{1}{2}\frac{1}{2})$		0.097	-0.144	-0.059	-0.11	-0.15 ± 0.08
$(\frac{1}{2}00)$	L	0.096	-0.207	-0.056	-0.17	-0.20 ± 0.06
	T	0.144	-0.158	-0.046	-0.06	-0.10 ± 0.02
(1 0 0)		0.270	-0.389	-0.078	-0.20	0.02 ± 0.05

In summary, perturbative calculations have been performed for the shift in frequencies of selected phonon modes in Mo. It is found that it is necessary to take into account angular forces arising from directional d-bonding in order to give a reasonable description of the anharmonic terms obtained from first-principles frozen phonon calculations. The results agree reasonably well with the available experimental data [5].

Acknowledgments

The authors would like to thank Professor C Stassis for many stimulating discussions. Ames laboratory is operated for the US Department of Energy by Iowa State University under contract no. W-7405-ENG-82. This research was supported by the Director for Energy Research, Office of Basic Energy Sciences including a grant of computer time at the supercomputer centre at Livermore Laboratory.

References

- [1] Srivastava G P and Weaire D 1987 *Adv. Phys.* **36** 463
Ho K-M and Harmon B N 1990 *Mater. Sci. Eng. A* **127** 155
- [2] Ho K-M, Fu C-L and Harmon B N 1984 *Phys. Rev. B* **29** 1575
- [3] Powell B M, Martel P and Woods A D B 1968 *Phys. Rev.* **117** 727; 1977 *Can. J. Phys.* **55** 1601
- [4] Muhlestein L D, Gurmen E and Cunningham R M 1972 *Inelastic Scattering of Neutrons* (Vienna: IAEA) p 53
- [5] Zarestky J, Stassis C, Harmon B N, Ho K-M and Fu C-L 1983 *Phys. Rev. B* **28** 697
- [6] Fu C-L and Ho K-M 1983 *Phys. Rev. B* **28** 5480
- [7] Ye Y-Y, Chen Y, Ho K-M, Harmon B N and Limdgård P A 1987 *Phys. Rev. Lett.* **58** 1769
- [8] Cowley R A 1968 *Rep. Prog. Phys.* **31** 123
- [9] Keating P N 1966 *Phys. Rev.* **149** 674
- [10] Ho K-M, Fu C-L and Harmon B N 1983 *Phys. Rev. B* **28** 6687
- [11] Fu C-L, Ho K-M, Harmon B N and Liu S H 1983 *Phys. Rev. B* **28** 2957
- [12] Singh D and Krakauer H 1991 *Phys. Rev. B* **43** 1441
- [13] Xu C H, Wang C-Z, Chan C-T and Ho K-M 1991 *Phys. Rev. B* **43** 5024